

Carrier-controlled ferromagnetism in SrTiO₃

Pouya Moetakef^{1,*}, James R. Williams^{2,*}, Daniel G. Ouellette³, Adam Kajdos¹, David Goldhaber-Gordon², S. James Allen³, and Susanne Stemmer^{1,}**

¹Materials Department, University of California, Santa Barbara, California, 93106-5050, USA

²Department of Physics, Stanford University, Stanford, California, 94305-4045, USA

³Department of Physics, University of California, Santa Barbara, California, 93106-9530, USA

* These authors contributed equally to the study.

** Corresponding author. Email: stemmer@mrl.ucsb.edu

Abstract

Magnetotransport and superconducting properties are investigated for uniformly La-doped SrTiO_3 films and $\text{GdTiO}_3/\text{SrTiO}_3$ heterostructures, respectively. $\text{GdTiO}_3/\text{SrTiO}_3$ interfaces exhibit a high-density two-dimensional electron gas on the SrTiO_3 -side of the interface, while for the SrTiO_3 films carriers are provided by the dopant atoms. Both types of samples exhibit ferromagnetism at low temperatures, as evidenced by a hysteresis in the magnetoresistance. For the uniformly doped SrTiO_3 films, the Curie temperature is found to increase with doping and to coexist with superconductivity for carrier concentrations on the high-density side of the superconducting dome. The Curie temperature of the $\text{GdTiO}_3/\text{SrTiO}_3$ heterostructures scales with the thickness of the SrTiO_3 quantum well. The results are used to construct a stability diagram for the ferromagnetic and superconducting phases of SrTiO_3 .

Two-dimensional electron liquids at interfaces between two insulating oxides, such as $\text{LaAlO}_3/\text{SrTiO}_3$, have generated tremendous excitement because of unique properties, such as strong electron correlations, superconductivity and ferromagnetism [1-4]. While superconductivity is a known bulk property of SrTiO_3 [5], ferromagnetism is not a property of either material and has so far only been observed for $\text{LaAlO}_3/\text{SrTiO}_3$ interfaces [3,6-9]. Furthermore, recent studies indicate the coexistence of superconductivity and ferromagnetism at these interfaces [6-8]. These observations raise a number of scientific questions. Among these, the most important question is whether ferromagnetism, and its coexistence with a superconducting state, is an intrinsic, many-body property of a two-dimensional oxide electron liquid in SrTiO_3 , or caused by extrinsic contributions, such as disorder, defects, or impurities [10]. Pointing to the latter are observations of ferromagnetic regions that form non-uniform patches [8], and inconsistencies in the appearance of magnetism in samples grown under the same conditions [11]. Furthermore, a large fraction of the interfacial charge at $\text{LaAlO}_3/\text{SrTiO}_3$ interfaces appears to be localized, indicating the presence of traps [12], and mobile charge densities are an order of magnitude less than what is needed to compensate for the polarization discontinuity [13].

In this study, ferromagnetism in SrTiO_3 , and its coexistence with superconductivity, are investigated in two different structures: extreme-electron-density electron liquids at $\text{GdTiO}_3/\text{SrTiO}_3$ interfaces and uniformly doped SrTiO_3 films. The charge carriers, which reside in the SrTiO_3 for both structures, have fundamentally different origins: for the uniformly doped SrTiO_3 films, La dopant atoms provide the carriers, while for the $\text{GdTiO}_3/\text{SrTiO}_3$ interfaces carriers are due to the interface. In particular, similar to $\text{LaAlO}_3/\text{SrTiO}_3$ interfaces, $\text{GdTiO}_3/\text{SrTiO}_3$ heterostructures exhibit a fixed polar charge, due to the dipole moment

associated with the $[\text{Gd}^{3+}\text{O}^{2-}/\text{Ti}^{3+}\text{O}_2^{4-}]$ bilayers along the (001) surface normal of GdTiO_3 . Unlike $\text{LaAlO}_3/\text{SrTiO}_3$, however, $\text{GdTiO}_3/\text{SrTiO}_3$ interfaces grown by molecular beam epitaxy (MBE) exhibit mobile carrier densities that are remarkably well predicted by the electrostatic requirements of the compensation of the polar discontinuity at the interface [14]. Carrier densities are $3\text{-}4 \times 10^{14} \text{ cm}^{-2}$, or $\sim 1/2$ electron per surface unit cell, *at each $\text{GdTiO}_3/\text{SrTiO}_3$ interface* for all heterostructures containing more than one unit cell of SrTiO_3 [14]. The staggered band alignment causes the mobile charge to reside in the SrTiO_3 , which is the wider band gap material [14]. These interfaces allow for doping of narrow SrTiO_3 quantum wells to extremely large and mobile carrier concentrations. For example, by sandwiching a few-unit-cell-thick SrTiO_3 layer between two GdTiO_3 layers, carrier concentrations in the SrTiO_3 approach one electron per site, conditions under which electron correlation effects should appear [15,16].

Here we show that both types of samples, uniformly doped SrTiO_3 films and high-density two-dimensional electron gases at $\text{GdTiO}_3/\text{SrTiO}_3$ interfaces, exhibit ferromagnetism. A ferromagnetic phase stability region appears on the high-density side of the superconducting dome in the phase diagram, and, at an intermediate carrier concentration, both phases coexist.

Three types of high-electron-concentration samples grown by MBE were investigated here: $\text{GdTiO}_3/\text{SrTiO}_3$ heterostructures grown on $(\text{LaAlO}_3)_{0.3}(\text{Sr}_2\text{AlTaO}_6)_{0.7}$ (LSAT) substrates, either containing a single electrically active interface ($\text{GdTiO}_3/\text{SrTiO}_3/\text{LSAT}$) or two active interfaces ($\text{GdTiO}_3/\text{SrTiO}_3/\text{GdTiO}_3/\text{LSAT}$), and two uniformly La-doped SrTiO_3 films of about 40 nm thickness (nominal dopant densities of $1 \times 10^{20} \text{ cm}^{-3}$ and $9 \times 10^{20} \text{ cm}^{-3}$, respectively) grown on LSAT substrates. Details of the MBE growth procedures have been described in detail elsewhere [14,17,18]. Previous studies have demonstrated a close correspondence between La dopant concentrations in the SrTiO_3 and mobile carrier densities, down to dopant concentrations

of $\sim 1 \times 10^{17} \text{ cm}^{-3}$ [19]. This provides evidence for the absence of additional sources of carriers, such as oxygen vacancies, and of traps such as transition metal impurities or Sr vacancies (which would reduce the carrier concentrations relative to the La dopant concentration), on the ppm level. Furthermore, positron annihilation studies of the La-doped films indicate Sr vacancy concentrations of no more than $\sim 1 \times 10^{16} \text{ cm}^{-3}$ in these films [20]. We note that the carrier densities in the uniformly doped samples investigate here are slightly less than the dopant concentration, because of the well-known surface depletion of SrTiO_3 [21]. For the $\text{SrTiO}_3/\text{GdTiO}_3$ heterostructures, the thickness of the SrTiO_3 layer was varied between 1 and 10 nm.

Ohmic contacts to the GdTiO_3 and SrTiO_3 layers were 300 nm Au/50 nm Ti and 300 nm Au/20 nm Ni/40 nm Al, respectively, with Au contact being the top-most layer in each case. Magnetoresistance measurements were carried out in Van der Pauw geometry using a Physical Properties Measurement System (Quantum Design PPMS). The sweep rates were varied between 0.005 and 0.01 T/s and all results (such as hysteresis and Curie temperature) shown here were found to be independent of the sweep rate. For the Hall measurements the magnetic field B was varied between ± 1 T. The two-dimensional (2D) carrier concentration n was calculated as $n = 1/(e \cdot R_H)$ where R_H is the measured 2D Hall coefficient. Low temperature measurements of the uniformly doped samples were performed in a dilution fridge, capable of temperatures down to 12 mK and magnetic field up to 9 T. The low temperature magnetoresistance was measured using a standard lock-in technique at a frequency of 13 Hz. Magnetization was measured using a SQUID magnetometer (Quantum Design Magnetic Properties Measurement System).

Figure 1(a) shows the longitudinal magnetoresistance, $R(B)$, where B is the magnetic field, of a 1-nm SrTiO₃ quantum well sandwiched between two GdTiO₃ layers, measured in four-terminal geometry. The sheet carrier density of this sample, as extracted from the Hall resistance, is $\sim 9 \times 10^{14} \text{ cm}^{-2}$ at room temperature and $\sim 1 \times 10^{15} \text{ cm}^{-2}$ at 5 K, corresponding to a three-dimensional (3D) carrier density of $\sim 1 \times 10^{22} \text{ cm}^{-3}$ in the 1-nm quantum well. Negative magnetoresistance is apparent at low temperatures (below 10 K), as has been previously reported for La-doped SrTiO₃ [22]. Concurrent with the appearance of negative magnetoresistance, $R(B)$ becomes hysteretic, indicating ferromagnetism, when the magnetic field was in-plane and perpendicular to the current. We use the appearance of hysteresis to define the Curie temperature of the ferromagnetic transition, T_{Cm} . We note that although extrinsic effects, the possibility of which is further discussed below, in ferromagnets may give rise to magnetoresistance hysteresis, the presence of a hysteresis nonetheless implies ferromagnetic ordering [23]. The shape of the hysteresis is very similar to that observed by Brinkman et al. for a LaAlO₃/SrTiO₃ interface [3]; however, here it occurs at almost an order-of-magnitude higher temperature than in ref. [3].

Heterostructures with a single interface and 1-nm SrTiO₃, which contain half the carrier density or less (sheet carrier densities of $4.6 \times 10^{14} \text{ cm}^{-2}$ at room temperature and $1.9 \times 10^{14} \text{ cm}^{-2}$ at 5 K; the latter corresponding to a 3D concentration of $1.9 \times 10^{21} \text{ cm}^{-3}$), also show ferromagnetic hysteresis, albeit at a lower T_{Cm} of about 3 K [Fig. 1(b)]. Samples with thicker (2 nm) SrTiO₃ layers did not show any magnetoresistance hysteresis above 2 K. In addition to the hysteresis in $R(B)$, all samples that exhibit hysteresis show an increase in resistance as the temperature is lowered, indicating a departure in the nature of conduction from conventional metallic systems [24]. For data from a sample with a slightly thinner SrTiO₃ layer, see ref. [24].

GdTiO₃ layers are ferrimagnetic [17,25] and it is therefore entirely conceivable that the magnetism of the carriers in the SrTiO₃ is induced by the proximity to the GdTiO₃. However, the following observations can also be made: (i) ferromagnetism is absent in samples with SrTiO₃ layers that are thicker than 2 nm, despite similar sheet carrier densities and proximity to the GdTiO₃; (ii) the Curie temperature of GdTiO₃ is substantially higher (~ 20 K, see Fig. 2) than T_{Cm} of any of the two-dimensional electron liquids investigated here; and (iii) ferromagnetism also appears in highly-doped bulk SrTiO₃, when no GdTiO₃ layer is present, albeit at much lower temperatures, as will be discussed next.

Figure 3 shows $R(B)$ for 44 nm-thick SrTiO₃, uniformly doped with La to a density of $9 \times 10^{20} \text{ cm}^{-3}$, measured at $T = 12$ mK. Here, B is applied perpendicular to the current and parallel to the growth direction (i.e. perpendicular to the (001) growth surface). Magnetoresistance hysteresis is evident for this sample. The hysteresis shape is very similar to that of the two-dimensional electron gases discussed above and to that at a LaAlO₃/SrTiO₃ interface [3]. The onset of the hysteresis occurs at $T_{\text{Cm}} = 700$ mK, substantially lower than that of the two-dimensional electron liquid of the GdTiO₃/SrTiO₃ samples. The carrier concentration is above the maximum density for which SrTiO₃ becomes superconducting [26]; hence only the ferromagnetic behavior is evident. La-doped SrTiO₃ samples with a reduced doping density of $1 \times 10^{20} \text{ cm}^{-3}$ (Fig. 4) lie in a regime where superconducting correlations are expected to be important [22,26]. In Fig. 4, evidence for both a superconducting-zero-resistance-state (defined by a transition temperature, T_{Cs}) and a ferromagnetic state is apparent. At 12 mK, sweeping B from negative to positive fields, two features indicative of the two states are measured: a sharp drop to $R(B) = 0$ below $B = -1.7$ T, followed by a departure from $R(B) = 0$ at $B = 0.2$ T (red curve in Fig. 4a). This departure from the zero-resistance state is hysteretic (Fig. 4b). The temperature

dependence of $R(B)$ (Fig. 4a) shows the evolution of the superconducting and ferromagnetic states and demonstrates that the two transition temperatures are different ($T_{Cs} = 315$ mK and $T_{Cm} = 500$ mK for this sample). At very low temperatures the superconducting ground state dominates and only a weak hysteresis is observed. As the temperature is increased, a slow transition to a ferromagnetic ground state is apparent. At 450 mK, only the hysteretic component of $R(B)$ remains. The magnetoresistance hysteresis of the La-doped SrTiO_3 samples shows that ferromagnetism occurs in SrTiO_3 even in the absence of any proximity to a ferrimagnetic layer and is thus a bulk property of SrTiO_3 at sufficiently high La doping concentrations. A third sample with an even lower La doping concentration ($3 \times 10^{19} \text{ cm}^{-3}$ grown on a SrTiO_3 substrate) only shows superconductivity below 100 mK and no ferromagnetism. Bulk doping of SrTiO_3 with La to higher carrier densities is possible [16,27], but to obtain the carrier densities of the quantum wells (up to $1 \times 10^{22} \text{ cm}^{-3}$ in this study), the material would be more appropriately described as Sr-doped LaTiO_3 , which is a well-known antiferromagnet [28,29]. LaTiO_3 , up to Sr-doping concentration of $\sim 10\%$, exhibits a weak, canted ferromagnetic moment [28]. Although even the highest La-doping concentration ($\sim 5\%$ La doping) in this study is far from this regime, it is possible that locally such weak ferromagnetic correlations exist.

Figure 5 summarizes the correlation between the 3D carrier concentration in SrTiO_3 and the ferromagnetic (this study) and superconducting transition temperatures (literature and this study). Data from both bulk and two-dimensional electron liquids is shown in the same graph. For the uniformly doped films, a ferromagnetic phase stability region appears on the high-density side of the superconducting dome in the phase diagram, and, for a range of carrier concentrations, both phases coexist, as was evident in Fig. 4. The results from these samples provide evidence that ferromagnetic phase of SrTiO_3 at sufficiently high La dopant

concentrations is likely *not* mediated by unintentional defects such as oxygen vacancies or Fe impurities. Impurity-related ferromagnetism typically persists to very high temperatures (see e.g., ref. [10]), which is different from what is observed here. The results from the uniformly doped films are consistent with recent reports of a field-induced Kondo effect in field-gated SrTiO₃ structures, which can be considered a precursor to the ferromagnetism at higher carrier densities [30]. When the data from the heterostructures and uniformly doped films are combined, as shown in Fig. 5, the ferromagnetism appears to depend strongly carrier concentration, even though carriers are introduced via two fundamentally different mechanisms (interface and conventional doping). However, more studies are needed to determine the degree to which the proximity to one or two GdTiO₃ interfaces, respectively, acts to increase the ferromagnetic transition temperature in the heterostructures, and to clarify the role of the La-dopants in the uniformly doped films.

Theoretical models of the ferromagnetism in doped SrTiO₃ should address the potential roles of band filling, Coulomb repulsion [31] and the coexistence with a superconducting state. Theory should consider the importance of the role of the degree of filling of different bands and subbands in the SrTiO₃ [6], which are derived from the three degenerate t_{2g} d -orbitals of Ti [32], the role of strain and band degeneracy (note that all samples that exhibited ferromagnetism were grown on LSAT, causing compressive biaxial stress in the SrTiO₃) as well as the shape of the observed hysteresis, in particular the decrease in resistance as the magnetic field reaches the coercive field. Finally, the dependence of ferromagnetism on the quantum well thickness in the SrTiO₃ heterostructures implies that electric field gating may be used to modulate both ferromagnetism and superconductivity.

The authors thank Leon Balents and Allan MacDonald for many useful discussions. P. M. thanks Tyler Cain and Clayton Jackson for help with the thin film growth experiments. S.S. acknowledges support by the DOE Office of Basic Energy Sciences (Grant No. DEFG02-02ER45994). P.M was supported by the U.S. National Science Foundation (Grant No. DMR-1006640). J. R. W. and D. G-G. acknowledge support by a MURI program of the Army Research Office (Grant No. W911-NF-09-1-0398) and D. G. O and S. J. A. by the MRSEC Program of the National Science Foundation under Award No. DMR 1121053.

References

- [1] A. Ohtomo, D. A. Muller, J. L. Grazul, and H. Y. Hwang, *Artificial charge-modulation in atomic-scale perovskite titanate superlattices*, Nature **419**, 378-380 (2002).
- [2] A. Ohtomo and H. Y. Hwang, *A high-mobility electron gas at the LaAlO₃/SrTiO₃ heterointerface*, Nature **427**, 423-426 (2004).
- [3] A. Brinkman, M. Huijben, M. Van Zalk, J. Huijben, U. Zeitler, J. C. Maan, W. G. Van der Wiel, G. Rijnders, D. H. A. Blank, and H. Hilgenkamp, *Magnetic effects at the interface between non-magnetic oxides*, Nature Mater. **6**, 493-496 (2007).
- [4] N. Reyren, S. Thiel, A. D. Caviglia, L. F. Kourkoutis, G. Hammerl, C. Richter, C. W. Schneider, T. Kopp, A. S. Ruetschi, D. Jaccard, M. Gabay, D. A. Muller, J. M. Triscone, and J. Mannhart, *Superconducting interfaces between insulating oxides*, Science **317**, 1196-1199 (2007).
- [5] J. F. Schooley, W. R. Hosler, and M. L. Cohen, *Superconductivity in semiconducting SrTiO₃*, Phys. Rev. Lett. **12**, 474-475 (1964).
- [6] D. A. Dikin, M. Mehta, C. W. Bark, C. M. Folkman, C. B. Eom, and V. Chandrasekhar, *Coexistence of Superconductivity and Ferromagnetism in Two Dimensions*, Phys. Rev. Lett. **107**, 056802 (2011).
- [7] L. Li, C. Richter, J. Mannhart, and R. C. Ashoori, *Coexistence of magnetic order and two-dimensional superconductivity at LaAlO₃/SrTiO₃ interfaces*, Nat. Phys. **7**, 762-766 (2011).
- [8] J. A. Bert, B. Kalisky, C. Bell, M. Kim, Y. Hikita, H. Y. Hwang, and K. A. Moler, *Direct imaging of the coexistence of ferromagnetism and superconductivity at the LaAlO₃/SrTiO₃ interface*, Nat. Phys. **7**, 767-771 (2011).

- [9] A. J. Millis, *Oxide Interfaces: Moment of magnetism*, Nat. Phys. **7**, 749-750 (2011).
- [10] D. A. Crandles, B. DesRoches, and F. S. Razavi, *A search for defect related ferromagnetism in SrTiO₃*, J. Appl. Phys. **108**, 053908 (2010).
- [11] M. R. Fitzsimmons, N. W. Hengartner, S. Singh, M. Zhernenkov, F. Y. Bruno, J. Santamaria, A. Brinkman, M. Huijben, H. J. A. Molegraaf, J. de la Venta, and I. K. Schuller, *Upper Limit to Magnetism in LaAlO₃/SrTiO₃ Heterostructures*, Phys. Rev. Lett. **107**, 217201 (2011).
- [12] M. Sing, G. Berner, K. Goss, A. Muller, A. Ruff, A. Wetscherek, S. Thiel, J. Mannhart, S. A. Pauli, C. W. Schneider, P. R. Willmott, M. Gorgoi, F. Schafers, and R. Claessen, *Profiling the Interface Electron Gas of LaAlO₃/SrTiO₃ Heterostructures with Hard X-Ray Photoelectron Spectroscopy*, Phys. Rev. Lett. **102**, 176805 (2009).
- [13] M. Huijben, A. Brinkman, G. Koster, G. Rijnders, H. Hilgenkamp, and D. H. A. Blank, *Structure-Property Relation of SrTiO₃/LaAlO₃ Interfaces*, Adv. Mater. **21**, 1665-1677 (2009).
- [14] P. Moetakef, T. A. Cain, D. G. Ouellette, J. Y. Zhang, D. O. Klenov, A. Janotti, C. G. V. d. Walle, S. Rajan, S. J. Allen, and S. Stemmer, *Electrostatic carrier doping of GdTiO₃/SrTiO₃ interfaces*, Appl. Phys. Lett. **99**, 232116 (2011).
- [15] M. Imada, A. Fujimori, and Y. Tokura, *Metal-insulator transitions*, Rev. Mod. Phys. **70**, 1039-1263 (1998).
- [16] Y. Tokura, Y. Taguchi, Y. Okada, Y. Fujishima, T. Arima, K. Kumagai, and Y. Iye, *Filling dependence of electronic properties on the verge of metal–Mott-insulator transition in Sr_{1-x}La_xTiO₃*, Phys. Rev. Lett. **70**, 2126-2129 (1993).

- [17] P. Moetakef, J. Y. Zhang, A. Kozhanov, B. Jalan, R. Seshadri, S. J. Allen, and S. Stemmer, *Transport in ferromagnetic GdTiO₃/SrTiO₃ heterostructures*, Appl. Phys. Lett. **98**, 112110 (2011).
- [18] B. Jalan, R. Engel-Herbert, N. J. Wright, and S. Stemmer, *Growth of high-quality SrTiO₃ films using a hybrid molecular beam epitaxy approach*, J. Vac. Sci. Technol. A **27**, 461-464 (2009).
- [19] J. Son, P. Moetakef, B. Jalan, O. Bierwagen, N. J. Wright, R. Engel-Herbert, and S. Stemmer, *Epitaxial SrTiO₃ films with electron mobilities exceeding 30,000 cm² V⁻¹ s⁻¹*, Nat. Mater. **9**, 482-484 (2010).
- [20] D. J. Keeble, B. Jalan, L. Ravelli, W. Egger, G. Kanda, and S. Stemmer, *Suppression of vacancy defects in epitaxial La-doped SrTiO₃ films*, Appl. Phys. Lett. **99**, 232905 (2011).
- [21] A. Ohtomo and H. Y. Hwang, *Surface depletion in doped SrTiO₃ thin films*, Appl. Phys. Lett. **84**, 1716-1718 (2004).
- [22] H. Suzuki, H. Bando, Y. Ootuka, I. H. Inoue, T. Yamamoto, K. Takahashi, and Y. Nishihara, *Superconductivity in single-crystalline Sr_{1-x}La_xTiO₃*, J. Phys. Soc. Jpn. **65**, 1529-1532 (1996).
- [23] M. Ziese, *Extrinsic magnetotransport phenomena in ferromagnetic oxides*, Rep. Prog. Phys. **65**, 143-249 (2002).
- [24] See supplemental material at [link to be inserted by publisher] for the resistance as a function of temperature and magnetoresistance data from a SrTiO₃/GdTiO₃/SrTiO₃ sample with a 0.8 nm thick quantum well.
- [25] H. D. Zhou and J. B. Goodenough, *Localized or itinerant TiO₃ electrons in RTiO₃ perovskites*, J. Phys.: Condens. Matter **17**, 7395–7406 (2005).

- [26] J. F. Schooley, W. R. Hosler, E. Ambler, J. H. Becker, M. L. Cohen, and C. S. Koonce, *Dependence of the Superconducting Transition Temperature on Carrier Concentration in Semiconducting SrTiO₃*, Phys. Rev. Lett. **14**, 305-& (1965).
- [27] B. Jalan and S. Stemmer, *Large Seebeck coefficients and thermoelectric power factor of La-doped SrTiO₃ thin films*, Appl. Phys. Lett. **97**, 042106 (2010).
- [28] C. C. Hays, J. S. Zhou, J. T. Markert, and J. B. Goodenough, *Electronic transition in La_{1-x}Sr_xTiO₃*, Phys. Rev. B **60**, 10367-10373 (1999).
- [29] Y. Okada, T. Arima, Y. Tokura, C. Murayama, and N. Mori, *Doping- and pressure-induced change of electrical and magnetic properties in the Mott-Hubbard insulator LaTiO₃*, Phys. Rev. B **48**, 9677-9683 (1993).
- [30] M. Lee, J. R. Williams, S. Zhang, C. D. Frisbie, and D. Goldhaber-Gordon, *Electrolyte Gate-Controlled Kondo Effect in SrTiO₃*, Phys. Rev. Lett. **107**, 256601 (2011).
- [31] J. Hubbard, *Electron Correlations in Narrow Energy Bands*, Proc. R. Soc. Lond. A **276**, 238-257 (1963).
- [32] L. F. Mattheiss, *Effect of the 110°K Phase Transition on the SrTiO₃ Conduction Bands*, Phys. Rev. B **6**, 4740-4753 (1972).
- [33] J. Appel, *Soft-Mode Superconductivity in SrTiO_{3-x}*, Phys. Rev. **180**, 508–516 (1969).

Figure Captions

Figure 1: (a) Magnetoresistance of a 4 nm GdTiO₃/1 nm SrTiO₃/4 nm GdTiO₃/LSAT heterostructure at 15 K, 10 K, 5 K, and 2 K. Hysteresis appears below ~ 10 K in sweeps with increasing and decreasing B, respectively (see arrows). (b) Magnetoresistance of a 8 nm GdTiO₃/1 nm SrTiO₃/LSAT heterostructure at 5 K and 2 K.

Figure 2: Magnetization as a function of temperature at 10 mT for a 4 nm GdTiO₃/1 nm SrTiO₃/4 nm GdTiO₃/LSAT heterostructure. The dashed line is a guide to the eye. The inset shows the magnetization M as a function of magnetic field at 2 K.

Figure 3. (a) Magnetoresistance of La-doped SrTiO₃ film with a carrier density of $9 \times 10^{20} \text{ cm}^{-3}$ at 12 mK, showing hysteresis during sweeps with increasing and decreasing B, respectively.

Figure 4. (a) Magnetoresistance of a La-doped SrTiO₃ film with a carrier density of $1 \times 10^{20} \text{ cm}^{-3}$ as a function of temperature, measured with increasing B field. (b) Magnified magnetoresistance at 12 mK. The hysteresis in sweeps with increasing and decreasing B (see arrows) indicates the coexistence of superconductivity and ferromagnetism.

Figure 5. Superconducting and ferromagnetic transition temperatures of SrTiO₃ as a function of carrier concentration. Literature data for the superconducting transition temperatures is from Appel et al. (ref. [33]). The sheet carrier densities of the quantum wells (n_{2D}) were converted to 3D carrier concentrations (n_{3D}) according to $n_{3D} = n_{2D}/t \text{ [cm}^{-3}\text{]}$, where t is the thickness of the quantum well and n_{2D} the carrier concentration determined from the Hall measurements at 5 K.

Figure 1

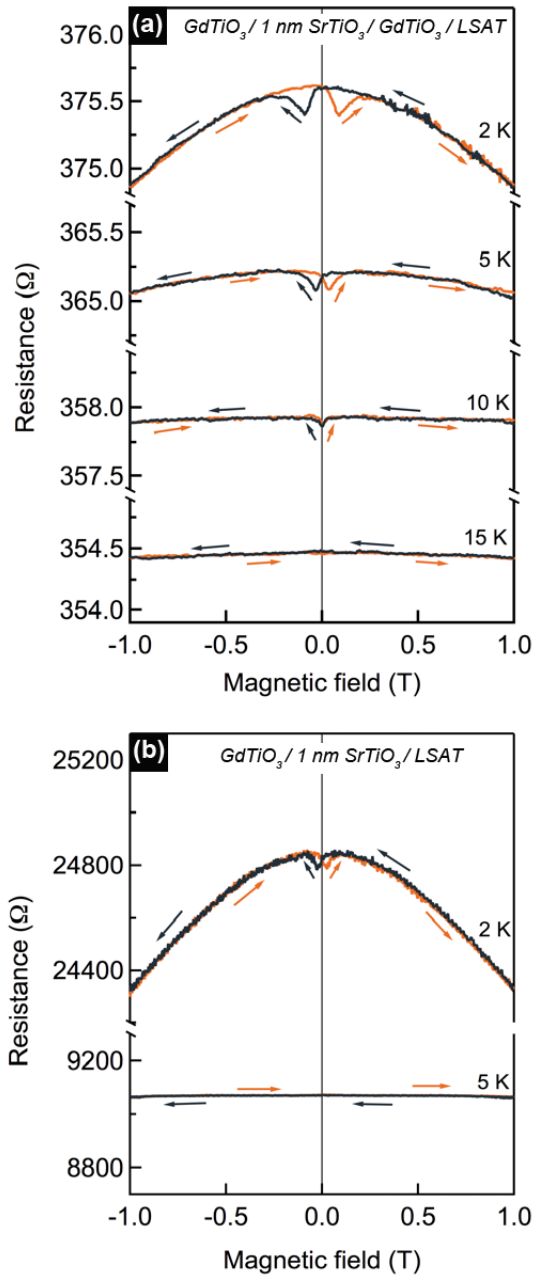


Figure 2

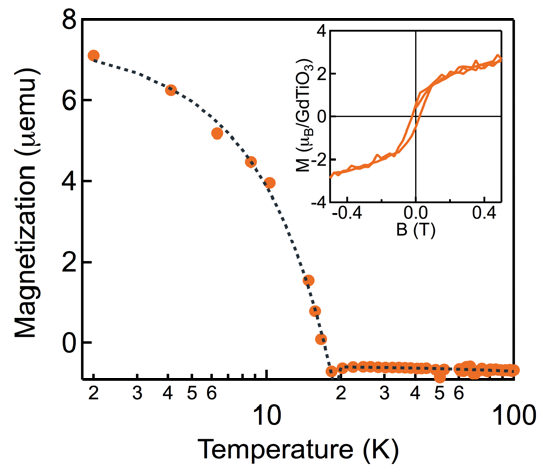


Figure 3

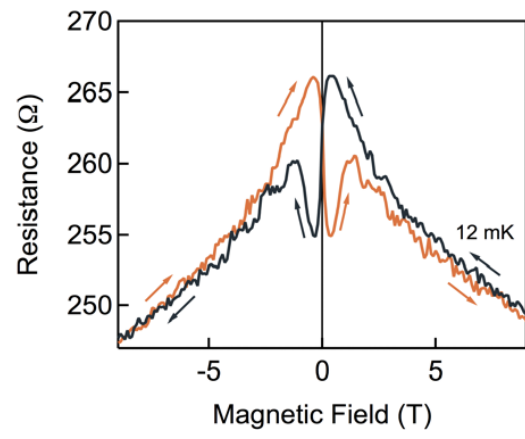


Figure 4

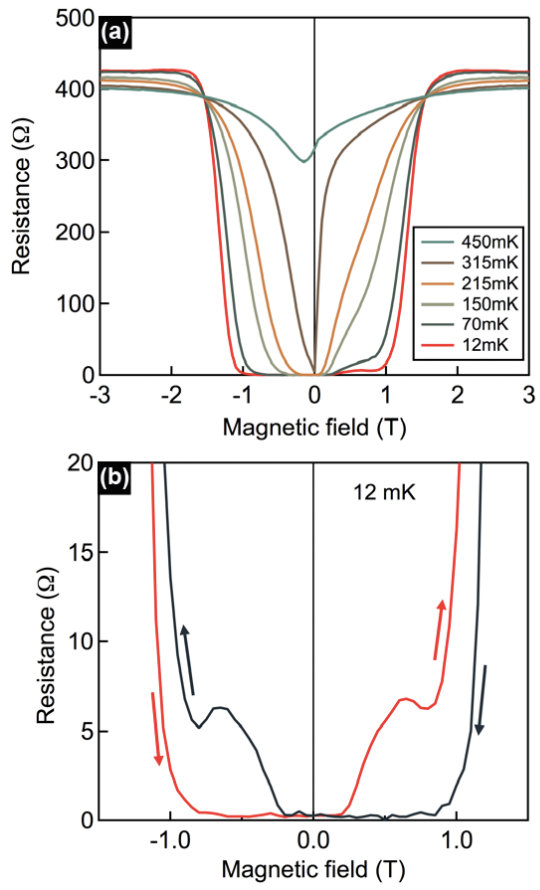
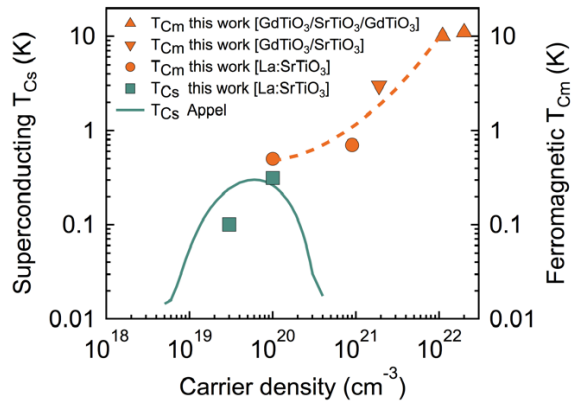


Figure 5



Supplementary information: Carrier-controlled ferromagnetism in SrTiO₃

Pouya Moetakef¹, James R. Williams², Daniel G. Ouellette³, Adam Kajdos¹, David Goldhaber-Gordon², S. James Allen³, and Susanne Stemmer¹

¹Materials Department, University of California, Santa Barbara, California, 93106-5050, USA

²Department of Physics, Stanford University, Stanford, California, 94305-4045, USA

³Department of Physics, University of California, Santa Barbara, California, 93106-9530, USA

Figure S1 shows the magnetoresistance of a 4 nm GdTiO₃/0.8 nm SrTiO₃/4 nm GdTiO₃/LSAT heterostructure at temperatures between 12 and 2 K. The carrier concentration for this sample at room temperature is $8.22 \times 10^{14} \text{ cm}^{-2}$ and at 2 K it is $1.52 \times 10^{15} \text{ cm}^{-2}$, corresponding to a 3D carrier concentration of $1.9 \times 10^{22} \text{ cm}^{-3}$.

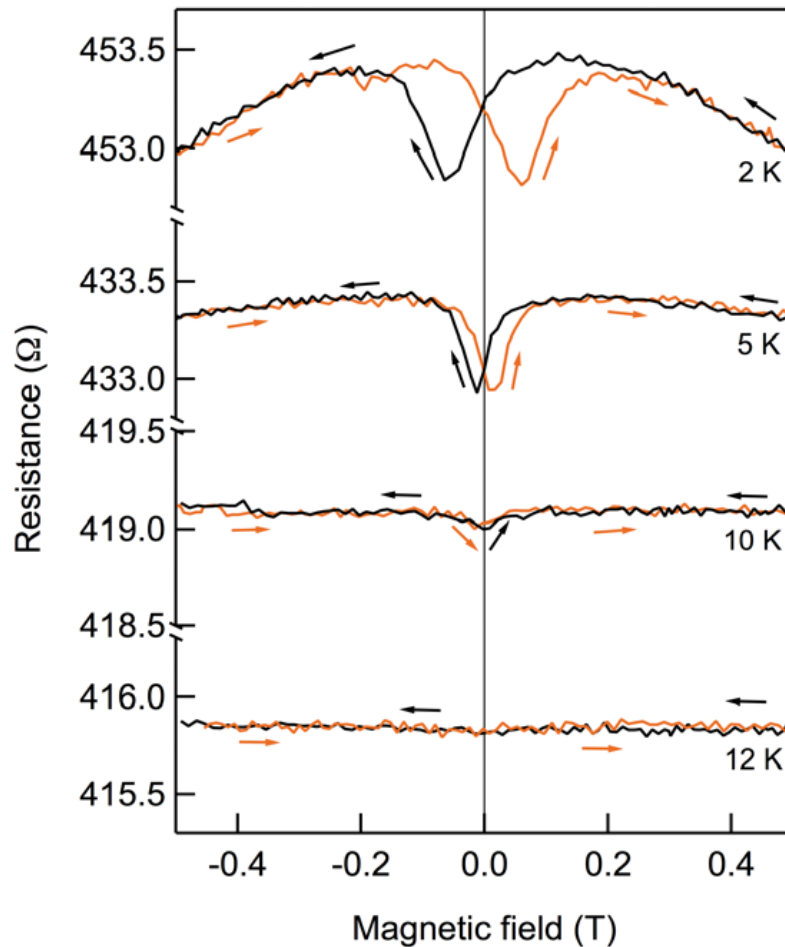


Figure S1: magnetoresistance of a 4 nm GdTiO₃/0.8 nm SrTiO₃/4 nm GdTiO₃/LSAT heterostructure at temperatures between 12 and 2 K. Hysteresis appears below ~ 10 K in sweeps with increasing and decreasing B , respectively (see arrows).

Figure S2 shows the sheet resistances and Hall carrier concentrations of the $\text{GdTiO}_3/1\text{-nm SrTiO}_3/\text{LSAT}$ and $\text{GdTiO}_3/1\text{-nm SrTiO}_3/\text{GdTiO}_3/\text{LSAT}$ heterostructures.

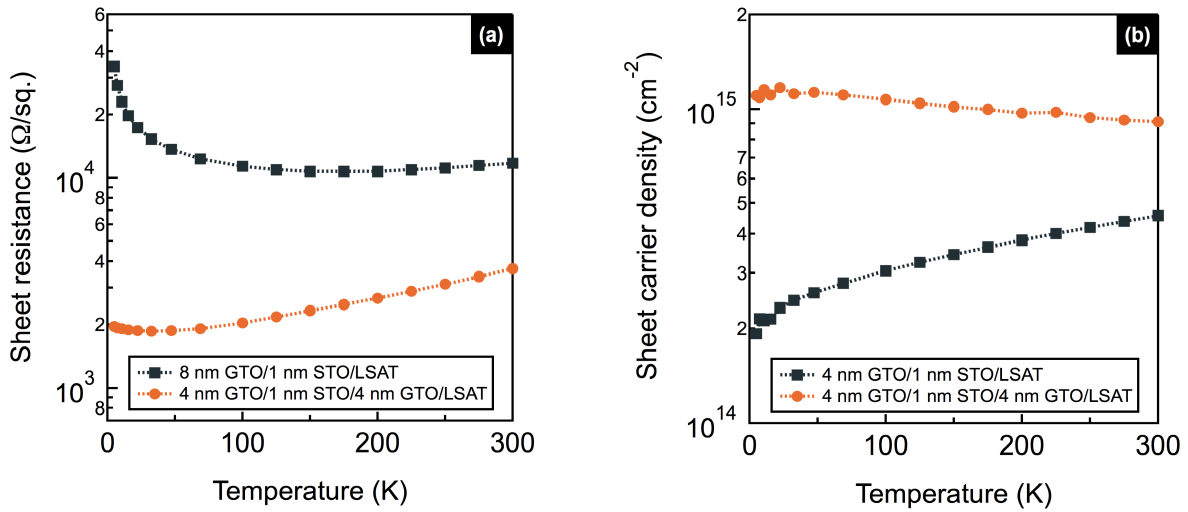


Figure S2: (a) Resistance and (b) carrier density as a function of temperature for two $\text{GdTiO}_3/\text{SrTiO}_3$ heterostructures.